

## Supplementary Materials for

### First-in-Human DR5 PET Reveals Insufficient DR5 Expression in GI Cancer

#### Patients

Shujing Wang<sup>1, #</sup>, Hua Zhu<sup>1, #</sup>, Yingjie Li<sup>2, #</sup>, Jin Ding<sup>1</sup>, Feng Wang<sup>1</sup>, Lixin Ding<sup>1</sup>,  
Xinyu Wang<sup>2</sup>, Jun Zhao<sup>2</sup>, Yan Zhang<sup>1</sup>, Yunfeng Yao<sup>2</sup>, Tong Zhou<sup>3</sup>, Nan Li<sup>1, \*</sup>, Aiwen  
Wu<sup>2, \*</sup>, Zhi Yang<sup>1, \*</sup>

<sup>1</sup>Key Laboratory of Carcinogenesis and Translational Research (Ministry of Education/Beijing), NMPA Key Laboratory for Research and Evaluation of Radiopharmaceuticals (National Medical Products Administration), Department of Nuclear Medicine, Peking University Cancer Hospital & Institute, Beijing 100142, China;

<sup>2</sup>Key Laboratory of Carcinogenesis and Translational Research (Ministry of Education/Beijing), Department of Gastrointestinal Surgery, Peking University Cancer Hospital & Institute, Beijing 100142, China;

<sup>3</sup>Department of Cell Biology and Divisions of Clinical Immunology and Rheumatology, University of Alabama at Birmingham, Birmingham, Alabama.

#### \* Correspondence to:

Dr Nan Li; rainbow6283@sina.com

Dr Aiwen Wu; wuaw@sina.com

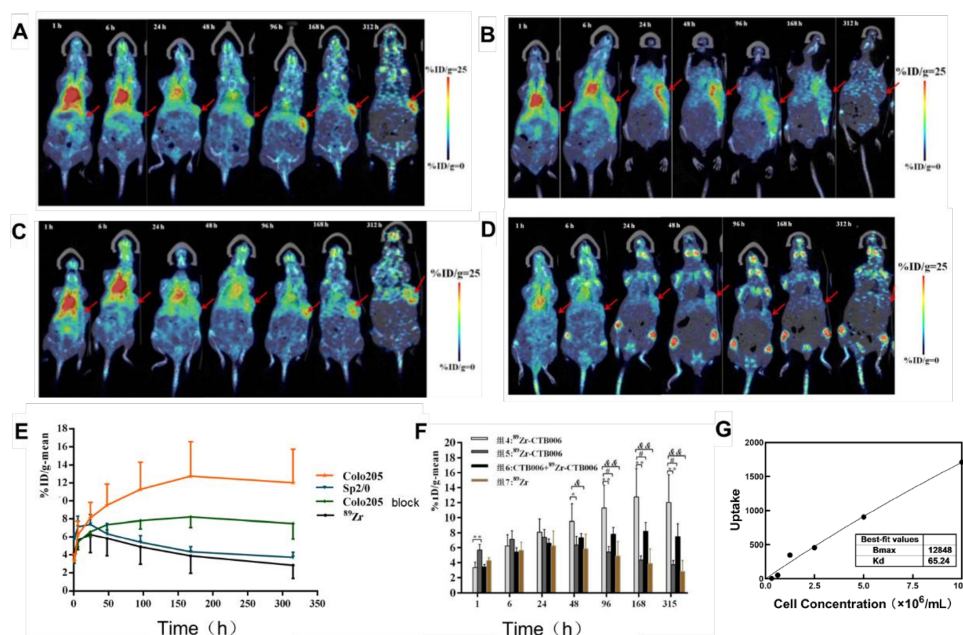
Dr Zhi Yang; pekyz@163.com

#### This PDF file includes:

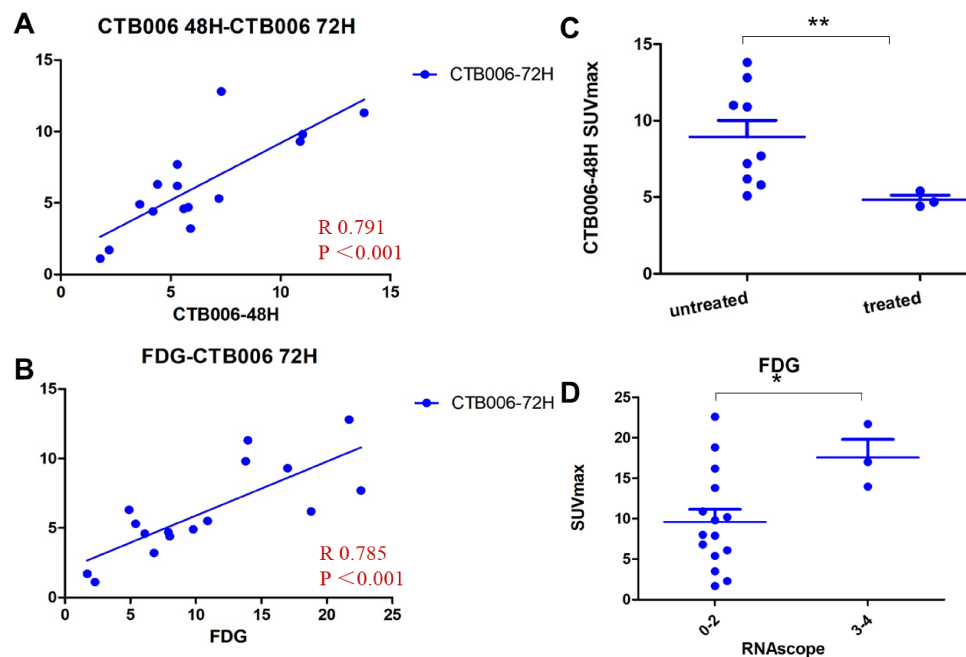
Figure S1 to S3

Figure S2 to S4

Figure S3 to S5  
Figure S4 to S6  
Figure S5 to S7  
Figure S6 to S8-9  
Table S1 to S10  
Table S2 to S11  
Table S3 to S12



**Figure S1.** The Colo205 tumor in the experiment group showed obvious uptake of  $^{89}\text{Zr}$ -CTB006 and obtained the highest uptake at 168h after administration (%ID/g:  $12.75 \pm 3.81$ ). The experiment group showed significant higher uptake in tumors than that in the blocking group (%ID/g:  $12.75 \pm 3.81$  vs  $8.21 \pm 1.16$ ,  $P < 0.05$ ), the control group (%ID/g:  $12.75 \pm 3.81$  vs  $4.34 \pm 0.55$ ,  $P < 0.01$ ) and the free  $^{89}\text{Zr}$  group (%ID/g:  $12.75 \pm 3.81$  vs  $3.88 \pm 1.93$ ,  $P < 0.01$ ). **A.** The PET/CT images of the Colo205 mouse in the experiment group. **B.** The PET/CT images of the Sp2/0 mouse in the control group. **C.** The PET/CT images of the Colo205 mouse in the blocking group. **D.** The PET/CT images of the Colo205 mouse in the free  $^{89}\text{Zr}$  group. **E-F.** The tumor %ID/g in the four groups. **G.** The affinity of  $^{89}\text{Zr}$ -CTB006 in Colo205 cells.



**Figure S2. A.** There was a significant positive correlation between the  $SUV_{max}$  of tumors on  $^{89}\text{Zr}$ -CTB006 PET/CT at 48h and that at 72h ( $P < 0.001$ ). **B.** There was a significant positive correlation between the  $SUV_{max}$  of tumors on  $^{89}\text{Zr}$ -CTB006 PET/CT at 72h and that on  $^{18}\text{F}$ -FDG PET/CT ( $P < 0.001$ ). **C.**  $SUV_{max}$  in colorectal cancer that had received radiotherapy or chemotherapy was significantly lower than that without treatment on 48h  $^{89}\text{Zr}$ -CTB006 PET/CT ( $4.83 \pm 0.51$  vs  $8.94 \pm 3.28$ ,  $P = 0.005$ ). **D.** The tumor uptake of  $^{18}\text{F}$ -FDG was also significantly higher in patients with RNAscope score 3-4 than that with score 0-2 ( $SUV_{max}$ :  $17.55 \pm 3.90$  vs  $9.60 \pm 6.05$ ,  $P = 0.046$ ).

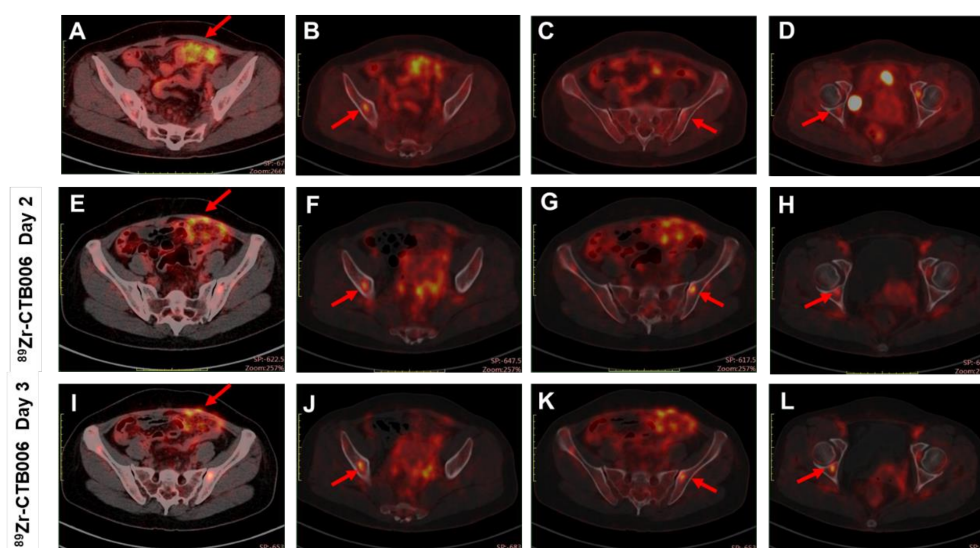


**Figure S3.**  $^{18}\text{F}$ -FDG PET/CT showed high uptake of the thickened peritoneum (**A**, arrow, SUVmax: 4.9) and the metastasis on the right iliac bone (**B**, arrow, SUVmax: 3.9), slight uptake of the metastasis on the left iliac bone (**C**, arrow, SUVmax: 2.1) and the right acetabulum (**D**, arrow, SUVmax: 2.1).  $^{89}\text{Zr}$ -CTB006 PET/CT showed inhomogeneous high uptake of the thicked peritoneum (**E**, arrow, SUVmax: 6.3 at 48h; **I**, arrow, SUVmax: 4.4 at 72h) and the metastases on the right iliac bone (**F**, arrow, SUVmax: 4.3 at 48h; **J**, arrow, SUVmax: 4.4 at 72h), the left iliac bone (**G**, arrow, SUVmax: 5.3 at 48h; **K**, arrow, SUVmax: 3.7 at 72h), the right acetabulum (**H**, arrow, SUVmax: 3.7 at 48h; **L**, arrow, SUVmax: 4.4 at 72h).

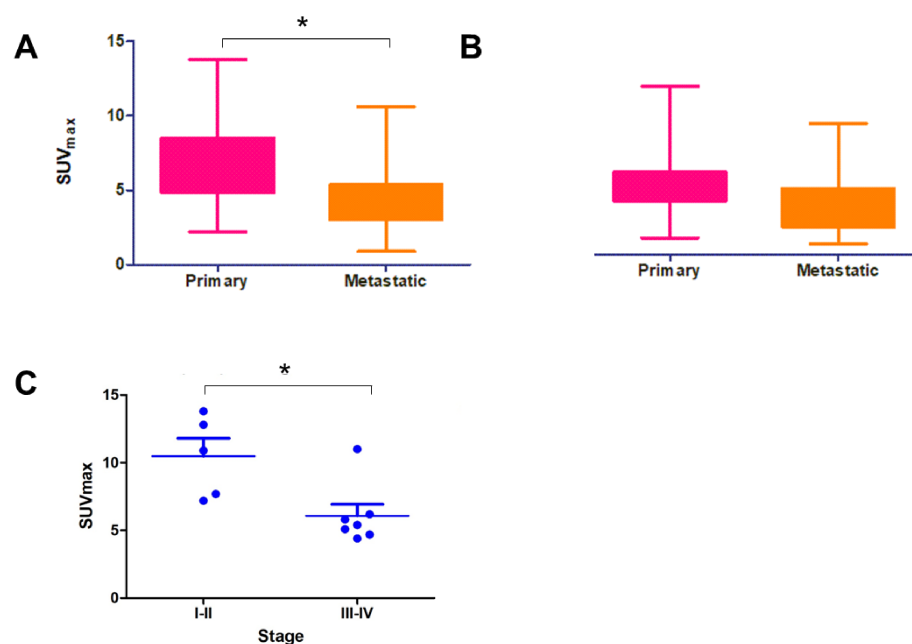


**Figure S4.** **A.** The uptake of  $^{89}\text{Zr}$ -CTB006 at 48h in the metastatic lesions was significantly lower than that in the primary lesions ( $6.97 \pm 3.14$  vs  $4.22 \pm 2.45$ ,  $P = 0.0135$ ). **B.** The uptake of  $^{89}\text{Zr}$ -CTB006 at 72h in the metastatic lesions was not significantly different from that in the primary lesions ( $5.18 \pm 2.63$  vs  $3.52 \pm 2.19$ ,  $P = 0.0704$ ). **C.** The uptake in colorectal cancer patients with III-IV stage was significantly lower than I-II stage ( $6.09 \pm 2.25$  vs  $10.48 \pm 2.96$ ,  $P = 0.015$ ).

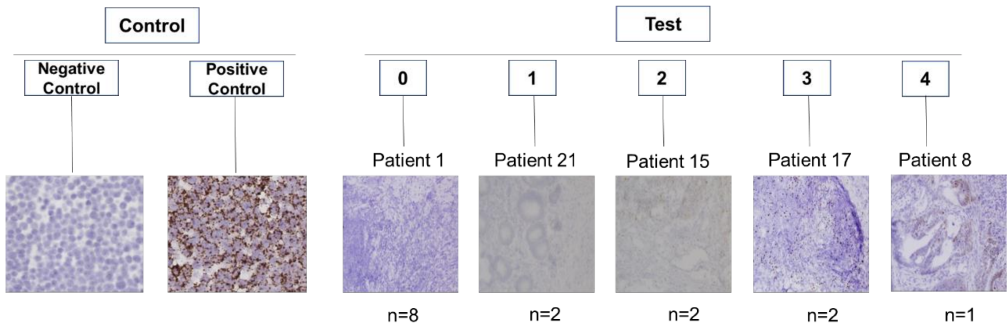


**Figure S5.** The negative and positive control images and the images of the representative sample with different RNAscope scores.

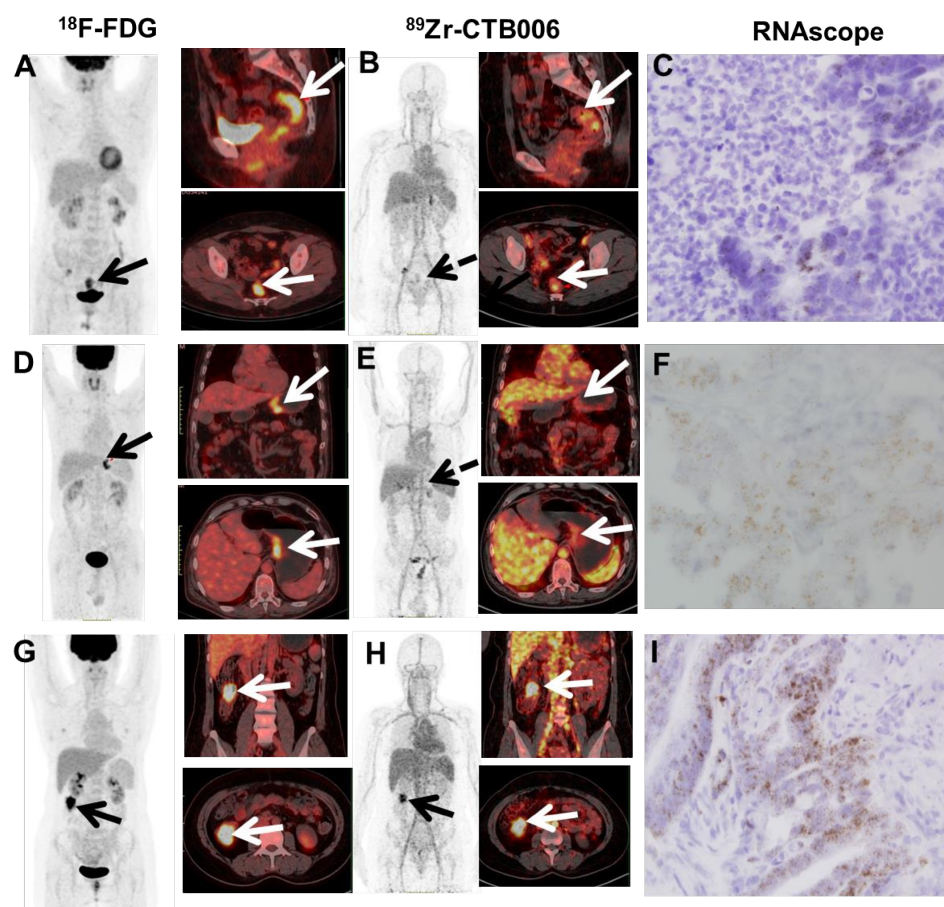


**Figure S6.** PET/CT images and RNAscope staining of patient 11, 15 and 8. **A.** MIP image, the axial and coronal PET-CT fused images of  $^{18}\text{F}$ -FDG PET/CT of patient 11 showed high uptake of  $^{18}\text{F}$ -FDG in tumor (arrow). **B.** MIP image, the axial and coronal PET-CT fused images of  $^{89}\text{Zr}$ -CTB006 PET/CT of patient 11 showed low uptake of  $^{89}\text{Zr}$ -CTB006 in tumor (arrow). **C.** RNAscope score of patient 11 was 1 (40X). **D.** MIP image, the axial and coronal PET-CT fused images of  $^{18}\text{F}$ -FDG PET/CT of patient 15 showed high uptake of  $^{18}\text{F}$ -FDG in tumor (arrow). **E.** MIP image, the axial and coronal PET-CT fused images of  $^{89}\text{Zr}$ -CTB006 PET/CT of patient 15 showed low uptake of  $^{89}\text{Zr}$ -CTB006 in tumor (arrow; the dash arrow indicates the unclearly tumor lesion). **F.** RNAscope score of patient 15 was 2 (40X).

**G.** MIP image, the axial and coronal PET-CT fused images of  $^{18}\text{F}$ -FDG PET/CT of patient 8 showed high uptake of  $^{18}\text{F}$ -FDG in tumor (arrow). **H.** MIP image, the axial and coronal PET-CT fused images of  $^{89}\text{Zr}$ -CTB006 PET/CT of patient 8 showed low uptake of  $^{89}\text{Zr}$ -CTB006 in tumor (arrow; the dash arrow indicates the unclearly tumor lesion). **I.** RNAscope score of patient 8 was 2 (40X).

**Table S1.** RNAscope Score

RNAscope score	Objective scoring by microscope
0	0 or less than 1 signal per 10 cells
1	1-3 signals per cell
2	4-10 signals per cell, very few cluster points
3	more than 10 signals per cell, positive cells with clusters are less than 10%
4	more than 10 signals per cell, positive cells with clusters are more than 10%

**Table S2.** Quality Control of  $^{89}\text{Zr}$ -CTB006 for Clinical Application

Parameter	QC specification	QC result
Appearance	Clear, colorless	Pass
Volume	1.5-2.5ml	2.5ml
Injection dose	18.5-74MBq	37MBq
pH	6.5-8.0	7.0
Radio-thin-layer	>95%	>99%
Chromatography		
Radio-high-performance	>95%	>99%
Liquid chromatography		
Ethanol	<5%	0
Endotoxins	<15EU/ml	Pass
Sterility	Sterile	Pass

**Table S3.**  $^{89}\text{Zr}$ -CTB006 Gender Averaged Organ Doses [mSv/MBq]

Target Organ	Effective Dose
Adrenals	8.77E-03
Brain	5.34E-04
Left colon	2.18E-02
Small Intestine	1.21E-03
Stomach Wall	7.63E-02
Heart Wall	8.66E-03
Kidneys	8.21E-03
Liver	5.68E-02
Lungs	6.61E-02
Ovaries	2.69E-03
Pancreas	5.60E-03
Prostate	2.72E-03
Salivary Glands	2.89E-04
Red Marrow	1.86E-02
Osteogenic Cells	8.86E-04
Spleen	1.08E-02
Urinary Bladder Wall	1.86E-03
Uterus	1.63E-03
Total Body	0.00E+00
Effective Dose	3.49E-01